

## Terahertz photoconductivity of $\text{Pb}_{1-x}\text{Sn}_x\text{Te}(\text{In})$

Dmitry Khokhlov,<sup>1,a)</sup> Ludmila Ryabova,<sup>1</sup> Andrey Nicorici,<sup>2</sup> Valery Shklover,<sup>3</sup> Sergey Ganichev,<sup>4</sup> Sergey Danilov,<sup>4</sup> and Vasily Bel'kov<sup>4,5</sup>

<sup>1</sup>*M. V. Lomonosov Moscow State University, Moscow 119991, Russia*

<sup>2</sup>*Institute of Applied Physics, Academy of Sciences of Moldova, Kishinev MD-2028, Moldova*

<sup>3</sup>*Swiss Federal Institute of Technology, Zurich CH-8083, Switzerland*

<sup>4</sup>*University of Regensburg, Regensburg D-93053, Germany*

<sup>5</sup>*A. F. Ioffe Physical-Technical Institute, St. Petersburg 194021, Russia*

(Received 19 November 2008; accepted 5 December 2008; published online 31 December 2008)

We have analyzed photoconductivity in  $\text{Pb}_{1-x}\text{Sn}_x\text{Te}(\text{In})$  under the action of  $\sim 100$  ns long terahertz laser pulses with the wavelength varying from 90 to 280  $\mu\text{m}$  in the temperature range 4.2–300 K. Strong photoresponse has been observed at all laser wavelengths used. Two types of photoresponse have been detected. Positive persistent photoconductivity, which is observed at  $T < 10$  K is due to photoexcitation of impurity states, whereas negative nonpersistent photoresponse prevailing at higher temperatures  $T \sim 25$  K results from free carrier heating. Specific features of photoconductivity mechanisms are discussed. © 2008 American Institute of Physics.

[DOI: 10.1063/1.3059572]

Terahertz physics and technology is one of the most rapidly growing areas of the modern physics. The progress in this field is advancing tremendously since it is important for many other areas of science, such as solid state physics, astrophysics, plasma physics, and others (see, e.g., Refs. 1–4). Furthermore, terahertz physics presents a potential for applications in medicine, environmental monitoring, high-speed communication, security, spectroscopy of different materials, including explosives, etc.<sup>3–6</sup> Development of detectors of laser radiation in this spectral range is one of the most challenging tasks. There are a number of possibilities, which include extrinsic photoconductivity detectors,<sup>7–9</sup> InAs (Putley) detectors,<sup>10</sup> pyroelectric detectors,<sup>2</sup> single electron device detectors,<sup>11</sup> and others. All of the terahertz photodetecting systems mentioned above have their advantages and shortcomings. Previously, we demonstrated that unique features of a narrow-gap semiconductor system-indium-doped  $\text{Pb}_{1-x}\text{Sn}_x\text{Te}$ -can be implemented for detection of terahertz radiation yielding extremely low noise equivalent power.<sup>12,13</sup> The detection is based on the extrinsic persistent photoconductivity periodically quenched by short radiofrequency pulses. A remarkable feature is that this material can be applied for detection in very long-wavelength range, where Ge(Ga) detectors are insensitive.

However the microscopic mechanisms of the photoconductivity in  $\text{Pb}_{1-x}\text{Sn}_x\text{Te}(\text{In})$  are not well understood so far.<sup>14</sup> Here we report on investigation of photoconductivity induced by short pulses of terahertz laser radiation in the wavelength range between 90 and 280  $\mu\text{m}$  in this material. We show that depending on temperature the mechanism of photoresponse is changing revealing persistent photoconductivity at low temperatures and fast subnanosecond photoresponse at higher temperatures. We present a microscopic picture of the mechanisms involved based on the analysis of the radiation intensity, temperature dependences, and kinetics of the photoconductivity.

The  $\text{Pb}_{1-x}\text{Sn}_x\text{Te}(\text{In})$  sample composition  $x=0.25$  and the doping level  $N_{In} \approx 0.5$  at. % were chosen in order to provide pinning of the Fermi level at 20 meV below the conduction band bottom and realization of a semi-insulating state at low temperatures.<sup>13</sup> Figure 1 shows temperature dependence of the sample resistivity  $\rho$ , free electron concentration  $n$ , and Hall mobility  $\mu$  taken in darkness, i.e., when the background radiation was completely screened out. Both resistivity and free electron concentration demonstrate activation behavior at  $T < 50$  K with the activation energy of 20 meV. The Hall mobility exceeds  $10^5$   $\text{cm}^2/\text{V s}$  at helium temperature and drops rapidly with temperature increasing. The dependence is characteristic of phonon-assisted scattering mechanism.<sup>15</sup> The samples were placed into an optical cryostat with  $z$ -cut crystal quartz windows, the sample temperature varied from 4.2 to 300 K. We note that due to windows, our samples were always exposed to thermal background radiation resulting in photogeneration of long-lived nonequilibrium free electrons at  $T < 25$  K and consequently, in lowering of material resis-

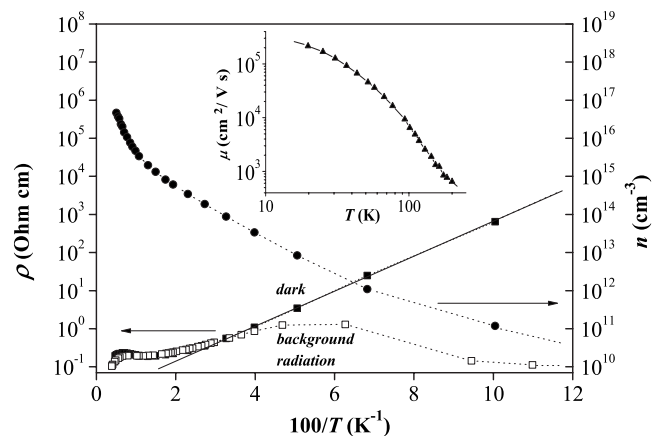


FIG. 1. Temperature dependence of the resistivity  $\rho$ , free electron concentration  $n$ , and Hall mobility  $\mu$  in  $\text{Pb}_{0.75}\text{Sn}_{0.25}\text{Te}(\text{In})$ . Solid symbols correspond to data taken in darkness, open symbols correspond to resistivity measured under the action of background illumination. Dashed lines are guides for eyes. The solid line corresponds to the resistivity activation behavior at  $T < 50$  K.

<sup>a)</sup>Electronic mail: khokhlov@mig.phys.msu.ru.

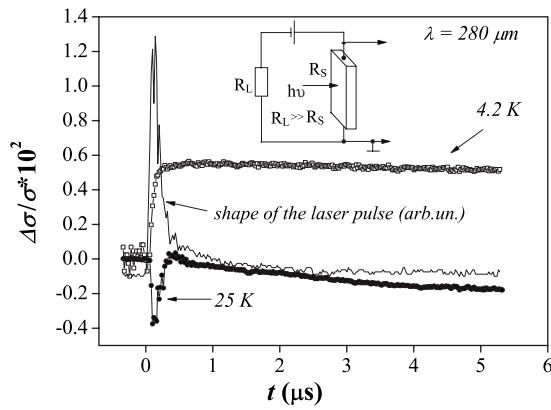


FIG. 2. Kinetics of the relative photoconductivity  $\Delta\sigma/\sigma$  under laser excitation at the wavelength of  $280\ \mu\text{m}$  taken at different temperatures. The laser pulse time profile is shown as well for a reference. The measurement circuit is shown in the insert.  $R_L$ , loading resistance and  $R_S$ , sample resistance.

tivity. The comparison of the two temperature dependences of resistivity taken in darkness and under the action of the background radiation is shown in Fig. 1. Photoconductivity was induced by  $\sim 100$  ns long pulses of an optically pumped  $\text{NH}_3$  terahertz laser<sup>2</sup> operating at 90, 148 or  $280\ \mu\text{m}$  wavelength with the power  $P$  up to 30 kW.

Irradiating samples by light at normal incidence, as sketched in the inset to Fig. 2, we observed a photoconductive signal at all wavelengths applied. Remarkable feature of the photoresponse is that its kinetics and even the sign depend on the temperature. Figure 2 shows kinetics of the relative photoconductivity  $\Delta\sigma/\sigma$  under excitation with a laser pulse at  $280\ \mu\text{m}$  wavelength for different temperatures. Here  $\sigma$  is the conductivity without laser illumination and  $\Delta\sigma$  is its change caused by the laser light. At the liquid helium temperature, the conductivity increases under the action of a laser pulse (positive photoconductivity). The photoresponse persists for the time much longer than the laser pulse length to at least several milliseconds. At temperatures above 25 K, in contrast, the photoconductivity becomes negative. Moreover at these conditions the signal follows the temporal structure of the applied laser pulse ( $\sim 100$  ns) indicating that the characteristic time of this negative photoconductivity is on the order of nanoseconds or less. This photoconductivity decreases rapidly with temperature rising vanishing at temperatures above 35 K. Such type of the photoconductivity kinetics was observed at all wavelengths of the incident laser radiation.

The positive and negative photoresponses have different dependence of their amplitudes on the laser power  $P$  (see Fig. 3). While the negative photoconductivity increases superlinearly with power rising and can be approximated by  $\Delta\sigma/\sigma \propto P^{1.3}$ , the positive photoconductivity saturates at high  $P$ . Figure 4 demonstrates that the observed long-term kinetics of the positive photoconductivity remains unchanged upon variation in the radiation power and is not simply due to depletion of impurity states responsible for the photoresponse.

The difference in signs and kinetics reveal two mechanisms of the photoconductivity. First, let us discuss photoconductivity observed at higher temperatures. Fast negative photoconductivity starts to prevail at  $T > 20$  K. The most well-known mechanism of negative photoconductivity corresponds to the heating of free electron gas under the action of

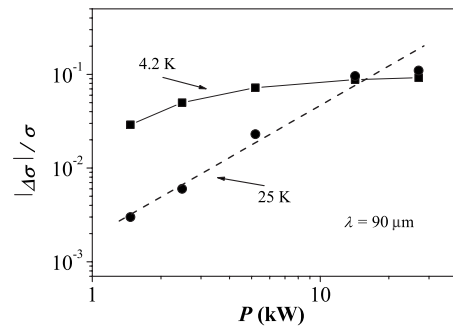


FIG. 3. Dependence of the relative photoresponse amplitude modulus  $|\Delta\sigma|/\sigma$  as a function of the laser power  $P$ , at different temperatures. The dashed line is a mean square fit of the data taken at 25 K corresponding to the power dependence  $|\Delta\sigma|/\sigma \propto P^{1.3}$ . The solid line is a guide for eyes.

a laser radiation resulting in the change of electron mobility. If it drops with temperature increasing (phonon-assisted scattering), as is observed experimentally (see Fig. 1), the photoconductivity signal is negative. Its kinetics is determined by the free carrier energy relaxation time, which is much shorter than the laser pulse length. The power dependence of the photoconductivity can be estimated from the temperature dependence of mobility and the signal magnitude. In our experiments, the maximal conductivity change induced by a laser pulse  $\Delta\sigma$  at, e.g., 25 K, is less than 10% of the initial conductivity value  $\sigma$  (see Fig. 3). Attributing this change to the variation in mobility, in the limit of a weak electron gas heating, the radiation-induced variation in conductivity may be approximated by<sup>2</sup>  $\Delta\sigma/\sigma = (1/\mu)(d\mu/dT_e)\Delta T_e$ , where  $\Delta T_e$  is the electron temperature change induced by a laser pulse. In the first approximation,  $\Delta T_e$  is proportional to the laser power  $P$ , so  $\Delta\sigma$  depends linearly on  $P$ . Experimentally, at  $T = 25$  K a somewhat stronger dependence  $\Delta\sigma \propto P^{1.3}$  is observed. We attribute this nonlinearity to the nonlinear temperature behavior of electron mobility in this temperature range.

Now we turn to the positive photoconductivity. The observed long-term kinetics demonstrates that it is due to the extrinsic photoconductivity, i.e., to photoexcitation of impurity states. Indeed, it is known that indium forms a set of impurity levels in the energy spectrum of  $\text{Pb}_{1-x}\text{Sn}_x\text{Te}(\text{In})$ . The ground impurity state provides pinning of the Fermi level in a position that is defined only by the alloy composi-

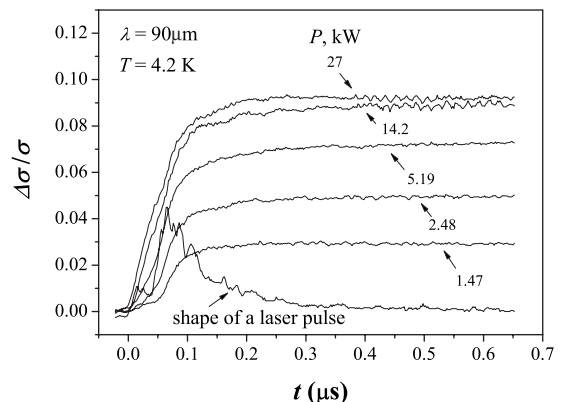


FIG. 4. Kinetics of the relative photoconductivity  $\Delta\sigma/\sigma$  under laser excitation at the wavelength of  $90\ \mu\text{m}$  taken for different peak power in laser pulses.  $T = 4.2$  K. The laser pulse time profile is shown as well for a reference.

tion and does not depend on the degree of In doping.<sup>13</sup> In  $\text{Pb}_{0.75}\text{Sn}_{0.25}\text{Te}(\text{In})$ , it is pinned in the gap, at  $\sim 20$  meV below the conduction band bottom resulting in realization of a semi-insulating state at low temperatures. At the same time, there exists a metastable impurity state separated by energy barriers both from the ground impurity state and a state of the system with a delocalized electron in the conduction band.<sup>14</sup> This metastable impurity state is responsible for the appearance of a number of nonequilibrium effects (for a review, see Ref. 12). The low temperature positive persistent photoconductivity is driven by photoexcitation of nonequilibrium electrons from metastable local impurity states and, consequently, leads to conductivity rise. The relaxation time of photoexcited free electrons back to metastable impurity states  $\tau$  is on the order of milliseconds at  $T=4.2$  K.<sup>12,16</sup> Therefore the photoresponse is persistent in the time scale of a laser pulse.

It should be taken into account that the background radiation was not screened out in our experiments. Hence the observed photoresponse corresponds to extra free electrons generated by a laser pulse on the background of about  $10^{17}$   $\text{cm}^{-3}$  long-lived free electrons photoexcited by thermal radiation of sample environment. Therefore this effect may be observed at high enough excitation power only. The latter circumstances may result in saturation of the photoresponse as a function of the laser power, as detected here (see Fig. 3). Besides, the calculated quantum efficiency of photogeneration is on the order of  $10^{-7}$ , whereas it was shown to be  $\sim 1$  in the case of weak signals and complete screening of the background radiation.<sup>17</sup>

The value of  $\tau$  decreases exponentially as the temperature grows above 10–15 K with a respective drop in the amplitude of the positive photoresponse.

In summary, we have observed positive persistent photoconductivity at  $T < 10$  K and negative photoconductivity at  $T > 20$  K in  $\text{Pb}_{1-x}\text{Sn}_x\text{Te}(\text{In})$  ( $x=0.25$ ) under strong terahertz laser pulses. The positive photoconductivity detected at low temperatures is due to photogeneration from the metastable impurity states. The negative photoresponse corresponds to the electron gas heating accompanied by a respective drop of the carrier mobility. The results are strongly

affected by the presence of background radiation. Screening of the background should increase the positive photoresponse by several orders of magnitude. Finally we note that the cut-off wavelength of the positive extrinsic photoresponse is not determined yet and we expect that it can be extended to much longer wavelengths.

The research described in this paper was supported in part by the grants of DAAD, DFG, Russian Foundation for the Basic Research (Grant Nos. 07-02-01406 and 08-02-90104) and Swiss National Science Foundation (Grant No. IB7320-110921/1).

<sup>1</sup>K. Sakai, *Terahertz Optoelectronics* (Springer, Berlin, 2005).

<sup>2</sup>S. D. Ganichev and W. Prettl, *Intense Terahertz Excitation of Semiconductors* (Oxford University Press, Oxford, 2006).

<sup>3</sup>*Terahertz Frequency Detection and Identification of Materials and Objects*, edited by R. E. Miles, X.-C. Zhang, H. Eisele, and A. Krotkus (Springer, Berlin, 2007).

<sup>4</sup>*Terahertz Science and Technology for Military and Security Applications*, edited by D. L. Woolard, J. O. Jensen, and R. J. Hwu (World Scientific, Singapore, 2007).

<sup>5</sup>T. Edwards, *Gigahertz and Terahertz Technologies for Broadband Communications (Satellite Communications)* (Artech House, Norwood, MA, 2000).

<sup>6</sup>*Electronic Devices and Advanced Systems Technology*, edited by D. L. Woolard, W. R. Loerop, and M. Shur (World Scientific, Singapore, 2003).

<sup>7</sup>E. L. Dereniak and G. D. Boreman, *Infrared Detectors and Systems* (Wiley, New York, 1996).

<sup>8</sup>J. Wolf and D. Lemke, *Infrared Phys.* **25**, 327 (1985).

<sup>9</sup>E. E. Haller, *Mater. Sci. Semicond. Process.* **9**, 408 (2006).

<sup>10</sup>A. Hadni, *Essentials of Modern Physics Applied to the Study of the Infrared* (Pergamon, London, 1967).

<sup>11</sup>K. Ikushima, Y. Yoshimura, T. Hasegawa, S. Komiyama, T. Ueda, and K. Hirakawa, *Appl. Phys. Lett.* **88**, 152110 (2006).

<sup>12</sup>D. Khokhlov, *Int. J. Mod. Phys. B* **18**, 2223 (2004).

<sup>13</sup>B. A. Volkov, L. I. Ryabova, and D. R. Khokhlov, *Phys. Usp.* **45**, 819 (2002).

<sup>14</sup>L. I. Ryabova and D. R. Khokhlov, *JETP Lett.* **80**, 133 (2004).

<sup>15</sup>Yu. I. Ravich, B. A. Efimova, and I. A. Smirnov, in *Semiconducting Lead Chalcogenides*, edited by L. S. Stil'bans (Plenum, New York, 1970).

<sup>16</sup>I. I. Zasavitskii, A. V. Matveenko, B. N. Matsonashvili, and V. T. Trofimov, *Sov. Phys. Semicond.* **20**, 135 (1986).

<sup>17</sup>D. R. Khokhlov, I. I. Ivanchik, S. N. Raines, D. M. Watson, and J. L. Pipher, *Appl. Phys. Lett.* **76**, 2835 (2000).